

A hybrid green light-emitting diode comprised of *n*-ZnO/(InGaN/GaN) multi-quantum-wells/*p*-GaN

C. Bayram,¹ F. Hosseini Teherani,² D. J. Rogers,² and M. Razeghi^{1,a)}

¹Center for Quantum Devices, Department of Electrical Engineering and Computer Science, Northwestern University, Evanston, Illinois 60208, USA

²Nanovation SARL, 103 bis Rue de Versailles, Orsay 91400, France

(Received 5 June 2008; accepted 2 August 2008; published online 27 August 2008)

Hybrid green light-emitting diodes (LEDs) comprised of *n*-ZnO/(InGaN/GaN) multi-quantum-wells/*p*-GaN were grown on semi-insulating AlN/sapphire using pulsed laser deposition for the *n*-ZnO and metal organic chemical vapor deposition for the other layers. X-ray diffraction revealed that high crystallographic quality was preserved after the *n*-ZnO growth. LEDs showed a turn-on voltage of 2.5 V and a room temperature electroluminescence (EL) centered at 510 nm. A blueshift and narrowing of the EL peak with increasing current was attributed to bandgap renormalization. The results indicate that hybrid LED structures could hold the prospect for the development of green LEDs with superior performance. © 2008 American Institute of Physics. [DOI: 10.1063/1.2975165]

Solid state lighting (SSL) holds the promise of a more energy-efficient, longer-lasting, more compact, and lower maintenance substitute for today's incandescent and fluorescent light sources. Since lighting currently represents about 22% of all electricity consumption, the adoption of SSL could significantly reduce greenhouse gas emissions.¹ Light-emitting diodes (LEDs), based on the InGaN alloy, are currently the most promising candidates for realizing SSL. InGaN is a direct wide bandgap semiconductor with an emission that can span the entire visible spectrum via compositional tuning. However, InGaN LED performance remains wavelength-dependent. Indeed, ultrabright and efficient blue InGaN-based LEDs are readily available² but the performance of InGaN-based green LEDs is still far from adequate for use in SSL.^{3,4}

The higher In content required in the active layers for green emission causes problems. First, the limited solubility of In in InGaN (Ref. 5) imposes a restricted growth window for the green-emitting InGaN active layer. Second, InGaN with high In content becomes unstable at elevated substrate temperature (T_s).⁶ Conventionally, a *p*-GaN layer is grown on top of an InGaN multi-quantum-well (MQW) active layer. The *p*-GaN layer is grown at significantly higher T_s than the InGaN MQW active layer in order to obtain high structural quality. This leads, however, to In leaking out of the active layers, which reduces the LED output.^{4,6} Thus, it is important to combat In diffusion in order to obtain InGaN-based green LEDs with superior performance.

ZnO is a wide bandgap material ($E_g=3.3$ eV) with a large exciton binding energy (60 meV). It has a low toxicity and the same wurtzite structure as GaN. The small in-plane lattice mismatch ($\sim 1.8\%$) with GaN makes ZnO a good candidate for integration in nitride devices.^{7,8} Recently, there have been many reports of ultraviolet emitters based on *n*-ZnO/*p*-GaN heterostructures.^{9–11} In this work, ZnO is adopted as the *n*-layer in a new kind of hybrid green LED.

In conventional GaN-based LEDs, the *p*-layer is deposited on top of the *n*-layer because the *n*-layer can be grown

with higher crystallographic and morphological qualities than the *p*-layer. In this work, we adopted an inverted LED structure employing a *n*-ZnO layer grown on top of (InGaN/GaN) MQW/*p*-GaN/AlN/sapphire. Through the use of pulsed laser deposition (PLD), a high quality *n*-ZnO layer could be grown at significantly lower T_s than is typically required for GaN growth in metal organic chemical vapor deposition (MOCVD). This approach could be beneficial, particularly for green light emitters, in which the high In content InGaN active layers are adversely affected by the high T_s required for the GaN growth. Furthermore, the refractive index of ZnO at 500 nm is 2.0 compared with 2.5 for GaN. Thus, lower critical angle loss is expected for light extraction through ZnO-capped LEDs. In this paper, we investigate the optical, structural, and electrical characteristics of these hybrid green LEDs.

The AlGaInN compounds were grown in an AIXTRON 200/4-HT horizontal flow low pressure MOCVD reactor. Trimethylaluminum (TMAI), trimethylgallium (TMGa), trimethylindium (TMIn), and bis(cyclopentadienyl)magnesium (DCpMg) were the metal organic cation precursors for Al, Ga, In, and Mg sources, respectively. Ammonia (NH₃) was used as the nitrogen source. Hydrogen was used as the carrier gas in the AlN and *p*-GaN layers.

p-GaN was grown on 600-nm-thick AlN on sapphire in order to improve the quality of the *p*-GaN. Rapid thermal annealing was realized at 1000 °C for 30 s in order to activate the Mg dopant. Hole carrier concentration was determined to be 7.8×10^{17} cm⁻³ by Hall effect measurements. The surface of the *p*-GaN was chemically cleaned before the regrowth of the InGaN/GaN MQWs. A five period MQW structure was grown in a nitrogen ambient. Each period consisted of a 2-nm-thick InGaN quantum well with a 4-nm-thick GaN barrier. Finally, a *n*-ZnO layer was grown on top of the (InGaN/GaN) MQW/*p*-GaN by PLD to complete the green LED.

ZnO was also simultaneously grown on sapphire for electrical characterization purposes. Room temperature (RT) Hall effect measurements were performed on the *n*-ZnO/sapphire in van der Pauw configuration with

^{a)}Electronic mail: razeghi@eecs.northwestern.edu.

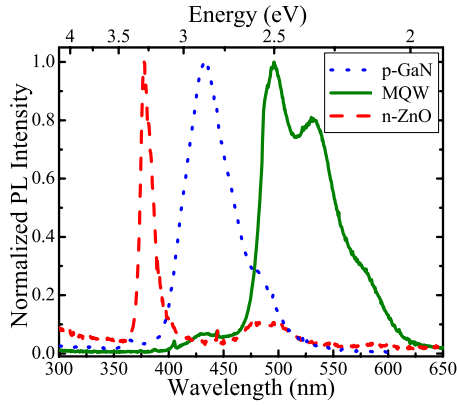


FIG. 1. (Color online) RT normalized PL spectra as consecutive *p*-GaN, InGaN/GaN MQW, and *n*-ZnO layers were grown on AlN/sapphire.

400 Å Ti/300 Å Pt/1200 Å Au contacts. The contacts proved Ohmic and carrier concentration was determined to be $2.8 \times 10^{19} \text{ cm}^{-3}$ with a mobility of $10.0 \text{ cm}^2/\text{V s}$ and a resistivity of $0.02 \text{ } \Omega \text{ cm}$.

Normalized RT photoluminescence (PL) spectra for the device layers are shown in Fig. 1. The spectrum for the *p*-GaN is dominated by 2.9 eV Mg-related peaks. This band is commonly observed in *p*-GaN and is attributed to defect-related deep level centers.¹² The PL spectrum, once the InGaN/GaN MQWs were grown on the *p*-GaN, shows a strong emission peaked at 2.5 eV without the 2.9 eV Mg-related peaks. The multiple peaks in the spectrum are generated by a Fabry-Pérot cavity formed with the AlN-sapphire interface. The PL spectrum for the completed hybrid LED structure (including the *n*-ZnO top layer) shows the strongest main emission peak centered at 3.3 eV. This corresponds to the ZnO band edge. The relative intensity of the 2.5 eV emission from the InGaN/GaN MQW in this spectrum is lower than that for the spectrum prior to ZnO growth. This is mainly due to the impact of the higher ZnO main emission peak intensity on the spectrum normalization.

Figure 2 shows an x-ray diffraction (XRD) ω - 2θ scan for the (0002) peak of the LED structure before- and after-ZnO growths. The ZnO and GaN peaks are indistinguishable suggesting a good lattice match. The full widths at half maximum (FWHMs) for the (0002) peaks before- and after-ZnO

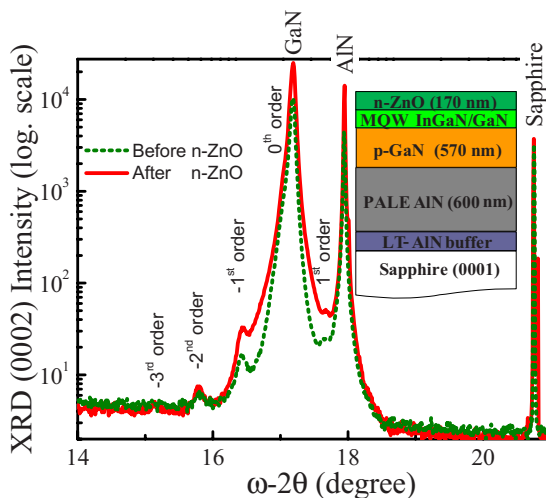


FIG. 2. (Color online) RT XRD ω - 2θ scans for the (0002) peak before and after growth of *n*-ZnO on the (InGaN/GaN) MQW/*p*-GaN/AlN/sapphire.

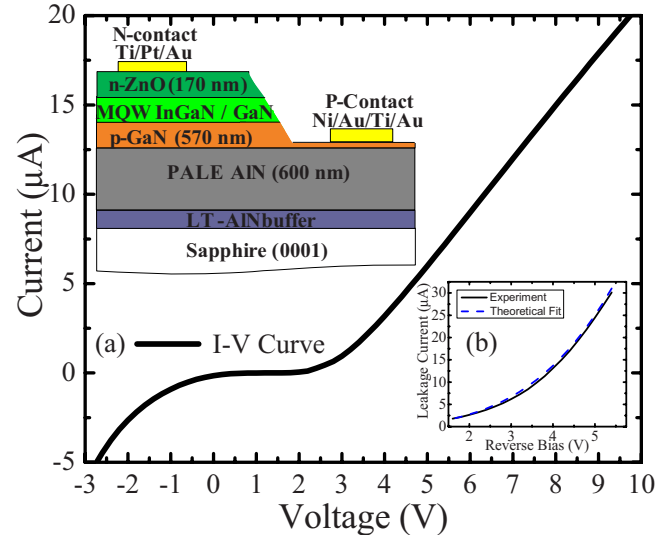


FIG. 3. (Color online) (a) *I*-*V* curve of the fabricated LED. The device structure is illustrated in the inset. (b) Leakage current vs reverse-bias voltage: Experimental and theoretical fits for the reverse-bias voltage range from -1.6 to -5.4 V .

depositions are 253 and 259 arc sec, respectively. The MQW-related satellite peaks were similar before and after the ZnO growth. This indicates that the active layers maintained their compositional and structural integrities. From the satellite peaks, the period of the active layer was determined to be 6.1 nm, which is in agreement with bulk growth calibrations.

Hybrid green LEDs were fabricated using conventional processing techniques. First of all, the samples were cleaned chemically. Then circular LED mesas with an area of 0.30 mm^2 were fabricated by masking the surface and dry etching right through the ZnO layer to a depth of 500 nm into the *p*-GaN. $30 \text{ } \text{Å}$ Ni/ $30 \text{ } \text{Å}$ Au/ $400 \text{ } \text{Å}$ Ti/ $1200 \text{ } \text{Å}$ Au and $400 \text{ } \text{Å}$ Ti/ $300 \text{ } \text{Å}$ Pt/ $1200 \text{ } \text{Å}$ Au contacts were evaporated onto the *p*-GaN and *n*-ZnO, respectively. The inset of Fig. 3(a) illustrates the device structure.

Figure 3(a) shows a typical *I*-*V* curve for a green-emitting hybrid LED. The turn-on voltage is around 2.5 V, which is close to the bandgap energy observed in the PL spectrum (Fig. 1). The on-series resistance (R_s) is calculated via a linear fit to the equation¹³ $IdV/dI = R_s I + kT/e$ for $V \gg kT/e$ and determined to be $4.75 \text{ M}\Omega$. This relatively high value is most likely due to (1) high contact resistance because the metal contacts to the *p*-GaN were not annealed and (2) the closeness ($\sim 70 \text{ nm}$) of the *p*-contact to GaN/AlN interface, which could lead to interface effects such as a two dimensional electron gas or elevated dislocation densities corrupting the Ohmic nature of the contact. R_s could be lowered through the use of a lower *p*-GaN etch depth to increase the separation between the contact and the GaN/AlN interface. The Ni/Au was not annealed to make a better Ohmic contact with the *p*-GaN because the ZnO surface morphology was observed to be modified by annealing at $500 \text{ } ^\circ\text{C}$. Decreasing the *p*-GaN etch depth and annealing the *p*-contact could improve the forward-bias (FB) *I*-*V* characteristics. Under FB, green light was easily observed with the naked eye at RT under continuous-wave operation.

Reverse-bias characteristics are zoomed in Fig. 3(b). As the *p*-GaN contact is close to the GaN/AlN interface, where

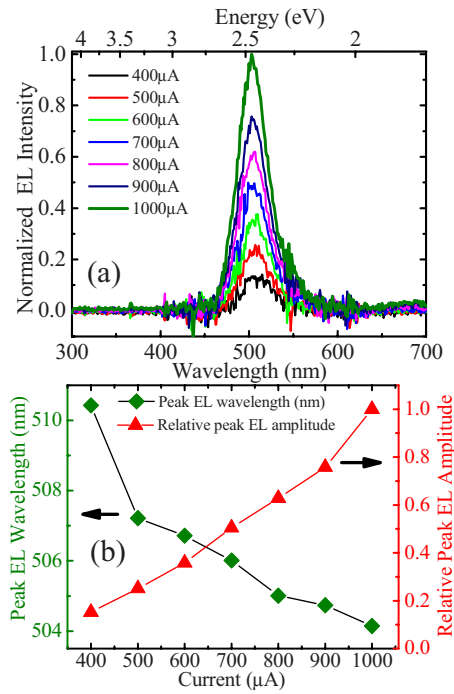


FIG. 4. (Color online) (a) Normalized EL intensity of the hybrid green LED at RT. (b) Peak EL wavelength and amplitude with respect to injection current.

there are many dislocations, a highly nonlinear increase in leakage current with respect to reverse-bias voltage was observed. The leakage current is known to be proportional to the square of the density of dislocations.¹⁴ At high reverse bias, there is field-assisted thermal ionization of carriers from the defect-associated traps, which is known as Poole–Frenkel effect. Thus, the leakage current is expected to obey^{15,16}

$$I = I_0 \exp\left(\frac{\beta_{\text{BF}} E^{1/2}}{kT}\right). \quad (1)$$

The average electric field (E) dependence on the reverse bias (V) was found from $E = (V + V_i)/w$, where V_i is the built-in junction voltage and w is the depletion width.^{15,17} Figure 3(b) plots the best fit of Eq. (1) to our experimental data. From this fit, we obtain $\beta_{\text{BF}} = 7.6 \times 10^{-4} \text{ eV V}^{1/2} \text{ cm}^{1/2}$. This value is slightly higher than for GaN ($4.5 \times 10^{-4} \text{ eV V}^{1/2} \text{ cm}^{1/2}$).¹⁶ For higher density of dislocations, β_{BF} tends to be bigger.^{14–16} Since leakage current scales with the square of the density of dislocations,¹⁴ the effective density of dislocations was calculated to be $8.2 \times 10^{-8} \text{ cm}^{-2}$. This theoretical fit shows that under reverse bias, hopping conduction is dominant in these hybrid LEDs similar to conventional p - n (In)GaN diodes.^{15,16} Further optimization of the hybrid LED design and fabrication process are in progress.

Electroluminescence (EL) spectra were acquired for the LEDs under pulsed operation (duty cycle of 10% and frequency of 5 kHz) in order to reduce heating effects under high current injection (Fig. 4). The peak intensity was observed to depend linearly on the current density [Fig. 4(b)]. A blueshift from 510 to 504 nm was observed as the current increased from 400 to 1000 μA . The FWHM decreased simultaneously from 194 to 179 meV. These effects have been attributed to free-carrier screening of the piezoelectric field, which leads to bandgap renormalization.¹⁸ The spectral nar-

rowing for the device demonstrates no band-filling effects even for higher current injections and thus indicates superior quality of the active layer.¹⁹ This is consistent with the high compositional and structural integrities of the MQWs inferred from the XRD studies and can be attributed to the lower T_s employed for PLD of the ZnO top n -layer.

In conclusion, ZnO was employed as the n -layer in an (In)GaN-based green LED with an inverted p - n structure. High crystallographic quality of the hybrid LED and the integrity of the MQWs were confirmed by XRD. The devices showed a turn-on voltage of 2.5 V, and a discrete green EL emission peaked at around 510 nm, which was visible to the naked eye. Thermally induced degradation of the InGaN active layers was combated through the adoption of PLD for the ultimate (n -ZnO) growth step since significantly lower T_s was required than for the conventional MOCVD growth of GaN. These results suggest that PLD-grown ZnO can be a good alternative to GaN for the n -layer in green LEDs. In addition, the inversion of the p - n junction such that the n -ZnO becomes the top layer, preserves the MQW and reduces the total internal reflection (which can improve light extraction).

The authors would like to acknowledge valuable fabrication support related to ZnO from J. Nguyen, K. Minder, Dr. S. R. Darvish, and Dr. J. L. Pau, all from Center for Quantum Devices.

¹C. J. Humphreys, MRS Bull. **33**, 459 (2008).

²N. F. Gardner, G. O. Muller, Y. C. Shen, G. Chen, S. Watanabe, W. Gotz, and M. R. Krames, Appl. Phys. Lett. **91**, 243506 (2007).

³Y. H. Cho, S. K. Lee, H. S. Kwack, J. Y. Kim, K. S. Lim, H. M. Kim, T. W. Kang, S. N. Lee, M. S. Seon, O. H. Nam, and Y. J. Park, Appl. Phys. Lett. **83**, 2578 (2003).

⁴I. K. Park, M. K. Kwon, J. O. Kim, S. B. Seo, J. Y. Kim, J. H. Lim, S. J. Park, and Y. S. Kim, Appl. Phys. Lett. **91**, 133105 (2007).

⁵I. Ho and G. B. Stringfellow, Appl. Phys. Lett. **69**, 2701 (1996).

⁶B. Daele, G. Van Tendeloo, K. Jacobs, I. Moerman, and M. R. Leys, Appl. Phys. Lett. **85**, 4379 (2004).

⁷D. J. Rogers, F. H. Teherani, A. Yasan, R. McClintock, K. Mayes, S. R. Darvish, P. Kung, M. Razeghi, and G. Garry, Proc. SPIE **5732**, 412 (2005).

⁸S. J. An, J. H. Chae, G. C. Yi, and G. H. Park, Appl. Phys. Lett. **92**, 121108 (2008).

⁹Ya. I. Alivov, J. E. Van Nostrand, and D. C. Look, Appl. Phys. Lett. **83**, 2943 (2003).

¹⁰D. J. Rogers, F. H. Teherani, A. Yasan, K. Minder, P. Kung, and M. Razeghi, Appl. Phys. Lett. **88**, 141918 (2006).

¹¹D. J. Rogers, F. H. Teherani, P. Kung, K. Minder, and M. Razeghi, Superlattices Microstruct. **42**, 322 (2007).

¹²M. Smith, G. D. Chen, J. Y. Lin, H. X. Jiang, A. Salvador, B. N. Sverdlov, A. Botchkarev, H. Morkoc, and B. Goldenberg, Appl. Phys. Lett. **68**, 1883 (1996).

¹³E. F. Schubert, Light-Emitting Diodes (Cambridge University Press, Cambridge, England, 2003).

¹⁴D. S. Li, H. Chen, H. B. Yu, H. Q. Jia, Q. Huang, and J. M. Zhou, J. Appl. Phys. **96**, 1111 (2004).

¹⁵D. V. Kuskonov, H. Temkin, A. Osinsky, R. Gaska, and M. A. Khan, Appl. Phys. Lett. **72**, 1365 (1998).

¹⁶M. S. Ferdous, X. Wang, M. N. Fairchild, and S. D. Hersee, Appl. Phys. Lett. **91**, 231107 (2007).

¹⁷S. M. Sze, Physics of Semiconductor Devices, 2nd ed. (Wiley, New York, 1981).

¹⁸T. Takeuchi, C. Wetzel, S. Yamaguchi, H. Sakai, H. Amano, and I. Akasaki, Appl. Phys. Lett. **73**, 1691 (1998).

¹⁹Y. D. Qi, H. Liang, D. Wang, Z. D. Lu, W. Tang, and K. M. Lau, Appl. Phys. Lett. **86**, 101903 (2005).